AIP Publishing

This manuscript was accepted by Appl. Phys. Lett. Click here to see the version of record.

Measurement of Mechanical Strain based on Piezo-Avalanche Effect

*Abbin Perunnilathil Joy, Mikhail Kanygin, and Behraad Bahreyni**

School of Mechatronic Systems Engineering, Simon Fraser University

250-13450, 102 Avenue, Surrey, BC, Canada V3T 0A3

ACCEPTED MANUSCRIPT

ABSTRACT

We are reporting on the use of the breakdown voltage of a pn junction to measure mechanical strain in micro-structures. The working principle relies on the dependence of silicon band gap to the mechanical stress which affects the current-voltage characteristics of the pn junction. An analytic model is developed and verified experimentally for the phenomenon. A micromechanical device with integrated junctions was designed and fabricated. Mechanical stress was applied onto the structure by subjecting it to mechanical vibrations. It is shown that the breakdown voltage of the device exhibited a high stress sensitivity of about $240\mu V/MPa$. The mechanical stress can also be measured by monitoring the device current while biased at a constant current. In this mode, the steep changes of the junction current in breakdown region led to nearly a tenfold higher stress sensitivity compared to a piezoresistive sensor. The high sensitivity, simple measurement, and potential for miniaturization for piezo-avalanche sensing make it a promising technique for measurement of stress in micro- and nano-mechanical devices.

AIP Publishing
This manuscript was accepted by Appl. Phys. Lett. Click here to see the version of record.

Sensors are used in various applications to monitor physical, chemical, or biological parameters and in an increasing number of cases, to provide awareness regarding the environment. Majority of sensors used in consumer applications, from mobile computing platforms to automotive and household systems, are fabricated based on micro-electro-mechanical systems (MEMS) technologies. A key factor behind the rapid spread of these microsensors is their low-cost that stems from their batch fabrication. These microsensors typically employ a micro-mechanical structure to convert the quantity of interest (e.g., acceleration) into a mechanical strain or displacement, which is further converted into a parameter that may be measured electrically (e.g., capacitance or resistance variations). While the designs of the micromechanical structures vary greatly based on the application, there are only a few transduction mechanisms that are commonly employed to convert the resultant strain or displacement into an electrical signal. Common transduction mechanisms at micro-scales include capacitive sensing for displacements [1] and piezoresistive [2] and piezoelectric [3] sensing for strain measurements. Employing each of these techniques brings up specific characteristics in terms of fabrication and usage. Capacitive sensing is a widely transduction mechanism employed due to its simple operating principle and fabrication. However, high-sensitivity capacitive transduction relies on lithographic resolution in most cases to create the narrow gaps and on deep etching techniques to realize high aspect-ratio trenches. As such, there are technological limits on the achievable performance and the costs of overcoming those barriers do not justify the improvements in the performance for many of the existing devices. Moreover, the nonlinearities often limit the dynamic range of capacitive sensors and necessitate a feedback loop. Piezoelectric devices offer very good performance for dynamic measurements but are unsuitable for the low-frequency measurements. As such, they are extensively used in high-frequency micro-transducers but are rarely used in much of the typical sensing applications for monitoring of slow-changing signals. On the other hand, the use of piezoelectric transductions requires the inclusion of a specific set of materials (e.g., aluminum nitride or various lead compounds) into the fabrication process, which is usually not feasible. Piezoresistive devices offer high linearity and sensitivity and have been employed widely. However, piezoresistive devices always require a current loop to measure resistance changes, which typically sets their minimum width (including the isolated paths to send and receive the current from the stressed location) to a multiple of lithographic/alignment resolution, hampering their utilization at small dimensions [4]. Integration of micromechanical and microelectronic devices has long been sought as a way of

ACCEPTED MANUSCRIPT

AIP Publishing

This manuscript was accepted by Appl. Phys. Lett. Click here to see the version of record.

direct conversion of signals from the mechanical domain to the electrical domain where researchers have embedded bipolar junction transistors [5], field effect transistors [6,7], and basic diodes [8,9] into the micro- or nano-mechanical structure. While these approaches provide high sensitivities to strain, they often complicate the fabrication process and may lower the overall manufacturing yield to the extent that the performance gains are offset by the additional cost of the final devices.

In this letter, we demonstrate the use of breakdown voltage of basic pn junctions for the highly-sensitive measurements of mechanical strain. The fabrication process is simple and relies on one doping step which can be carried in most standard processes. Additionally, using breakdown voltage for stress measurement allows for sensor optimization where the junction can be placed at the stressed location while contacts to the two sides of the junction can be made far from the junction itself. Also, the junction itself can be made as small as technologically possible (i.e., the lithographic resolution to open doping windows in mask layers), allowing precise measurement of stress at exact locations. Furthermore, access to a floating device (as needed for bridged piezoresistors) is no longer necessary, allowing measurements with a single contact to one side of the junction while sharing the other side between different stress sensors.

It is known that the mechanical stress affects several of the electrical properties of pn junctions reversibly [10–12]. While this stress-dependence can present challenges, e.g., the undesired response to packaging stresses, it has also been employed to develop sensors as well as to enhance the desired electronic properties of semiconductors. Effective mass, mobility, and lifetime of carriers, among other semiconductor properties, change in presence of mechanical stress [13]. Existing models and experimental verifications confirm a higher bulk electron mobility for strained silicon [14,15]. Another major effect of the mechanical stress is the narrowing of bandgap [16]. In silicon, an applied mechanical strain not only shifts the valence band edge but can also split it into two energy levels if the strain exceeds beyond a certain level [17]. The edge of conduction band, on the other hand, also shifts in response to the strain. Based on the deformation potential theory, the changes in bandgap, E_g, are proportional to the applied mechanical stress, σ:

$$E_g(\sigma) = E_{g0} + \alpha\,\sigma \quad (1)$$

ACCEPTED MANUSCRIPT

AIP Publishing
This manuscript was accepted by Appl. Phys. Lett. Click here to see the version of record.

where E_{g0} is the material bandgap at rest and α is a property of the semiconductor material ($\alpha = -1.5 \times 10^{-11} eV/Pa$ for Silicon) [18]. On the other hand, the carrier concentration is a function of the bandgap. It follows from Equation (1) that the changes in carrier concentration can be found from:

$$\Delta N_B = N_{B0}\left(1 - e^{-\frac{\alpha\,\sigma}{2k_BT}}\right) \tag{2}$$

where k_B is the Boltzmann constant, T is the temperature, and N_{B0} is the career concentration at rest. In semiconductor materials and junctions, the dependence of electrical properties of the material on the applied stress has been studied extensively and utilized to build sensors based on the piezojunction and piezoresistive effects from regular, compound, and organic semiconductors [19–21]. In case of pn junctions, the diode saturation current depends on mechanical stress [8,22]. In this work, we demonstrate that the exponential increase in diode current near breakdown region can be employed to measure mechanical stress with significantly higher sensitivity compared to basic piezojunction or piezoresistive measurements.

For highly doped junctions, Zener breakdown becomes the dominant mechanism. Due to the narrow depletion region width, the electric field across such junctions is significantly higher, which allows the charge carriers to tunnel through the potential barrier of the junction under a large enough reverse bias (typically 3-5V). It is expected that as the energy gap decreases under the applied stress, the electric field required to let the valence electrons to tunnel to the conductive band decreases. Consequently, the Zener breakdown voltage is expected to decrease under an applied load.

Avalanche breakdown is the dominant breakdown mechanism for lightly doped junctions ($N_B < {\sim}5 \times 10^{17} cm^{-3}$ or $V_{BR} > {\sim}5V$) and occurs due to the impact ionization of atoms within the depletion region under high electric fields [23]. While the dependence of the breakdown voltage on stress, herein referred to as the *piezo-avalanche effect*, has been observed before [24,25], it has not been employed in device designs despite its potential for sensitive measurements of stress. Moreover, an analytic model to relate the mechanical stress and breakdown voltage has not been developed.

ACCEPTED MANUSCRIPT

AIP Publishing

This manuscript was accepted by Appl. Phys. Lett. Click here to see the version of record.

A simple model for the dependence of the breakdown voltage can be developed. The breakdown voltage for an abrupt junction can be found from [23]:

$$V_{BR} = \frac{\varepsilon_s}{2qN_B}\mathcal{E}_m^2 \tag{3}$$

where N_B is the dominant carrier concentration, q is the electron charge, ε_s is the permittivity of the semiconductor, and $\mathcal{E}_m$ is the critical electric field. Most theories assume that the ionization field is equal to the band gap energy. However, it was found that a better fit of theory to experimental data could be achieved if energy of ionization is taken to be slightly larger as given by [26]:

$$\mathcal{E}_m = \frac{9.0680 \times 10^{13}}{\sqrt{\varepsilon_s}} N_B^{1/8}\, E_g^{3/4} \tag{4}$$

Finally, the dependence of changes in pn junction breakdown voltage on an applied stress can be found from:

$$\frac{\Delta V_{BR}}{V_{BR0}} = \frac{V_{BR0} - V_{BR}(\sigma)}{V_{BR0}} = 1 - \left(1 + \frac{\alpha\,\sigma}{E_{g_0}}\right)^{\frac{3}{2}} e^{-\frac{3\,k_B T}{8\,\alpha\,\sigma}} \approx -\alpha\left(\frac{3}{2E_{g0}} + \frac{3}{8k_B T}\right)\sigma \tag{5}$$

where V_{BR0} is the breakdown voltage of the unstressed structure. The difference between the nonlinear and linearized models in Equation 5 is small for typical values of mechanical stress encountered at small scales (e.g., about 1% for a 100MPa stress). Thus, the piezo-avalanche effect can be considered as a linear transduction mechanism for most sensing applications. As expected, both the breakdown voltage and its changes due to stress depend on the background doping concentrations (see Figure 1). However, as can be seen from equation 5, the sensitivity normalized to the unstressed breakdown voltage is independent of dopant concentration and is essentially set by the material properties.

ACCEPTED MANUSCRIPT

AIP Publishing

This manuscript was accepted by Appl. Phys. Lett. Click here to see the version of record.

To validate the theoretical model, a microdevice was fabricated and characterized through bulk micromachining of a silicon-on-insulator (SOI) substrate with a 2μm thick silicon device layer above a $1\mu m$ buried oxide layer. The device layer was blanked doped with Boron to establish a well-defined resistivity of $\sim 0.15\Omega - cm$ across the wafer, corresponding to a background boron concentration of $\sim 2 \times 10^{17} cm^{-3}$. Thermal oxidation, which also served as the annealing step for the implanted boron atoms, was employed to grow a 230nm silicon dioxide layer on the wafer surface. The oxide layer was then patterned through optical lithography to open up windows for a subsequent doping step. Phosphorous was then implanted to result in a $\sim 600nm$ junction depth below the surface. A $200nm$ low-stress layer of silicon nitride was then deposited for electrical isolation through a low-pressure chemical vapor deposition (LPCVD) step. The silicon nitride layer was then patterned in a reactive ion etching (RIE) process to create vias to the silicon surface. A high-quality, bilayer of aluminum-silicon alloy ($Al_{0.99}Si_{0.1}$) and nickel was deposited and patterned through a lift-off process. A blanket metal layer was also deposited on the backside of the wafer after removal of the dielectric layers. A deep reactive ion etch (DRIE) process was then

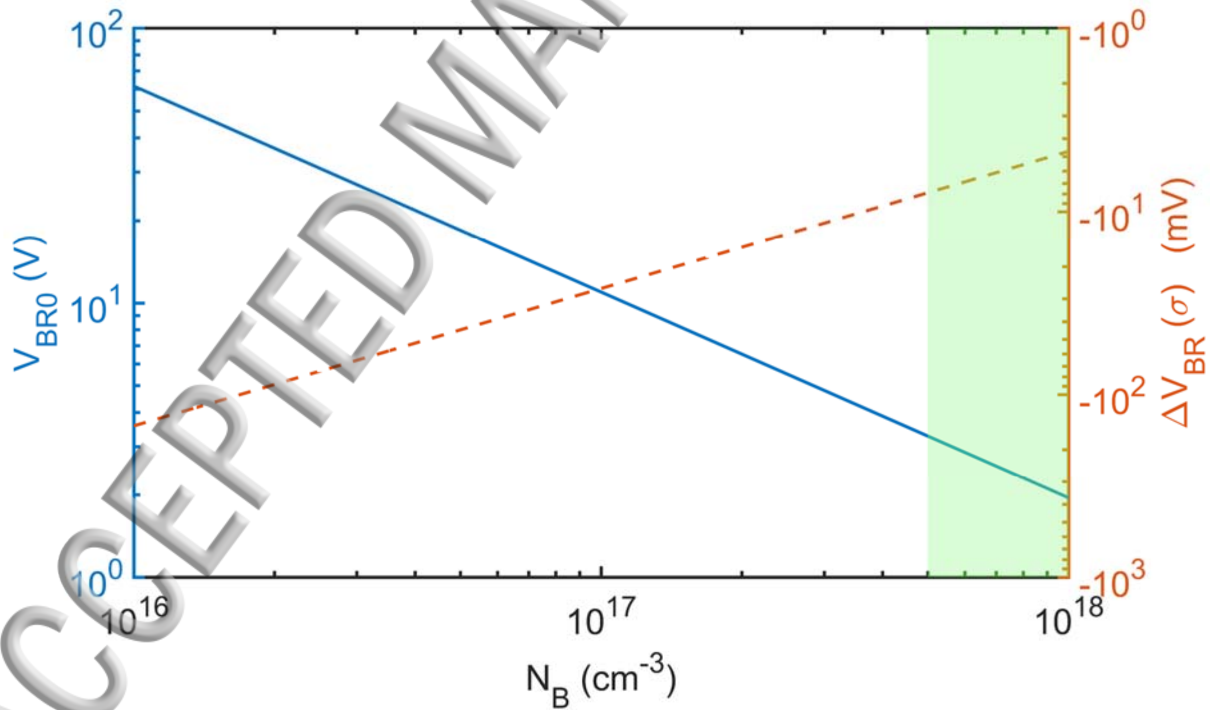

Figure 1. Dependence of the breakdown voltage and the sensitivity of the breakdown voltage to stress (i.e., $\Delta V_{BR}(\sigma) = V_{BR}(\sigma) - V_{BR0}$ for a given $\sigma = 10MPa$) on dopant concentration. Note that at high dopant concentrations (i.e., for $N_B > \sim 5 \times 10^{17} cm^{-3}$ as shaded on the graph) the dominant breakdown mechanism will gradually switch to Zener breakdown.

ACCEPTED MANUSCRIPT

AIP Publishing

This manuscript was accepted by Appl. Phys. Lett. Click here to see the version of record.

employed to pattern the 2μm device layer, stopping on the buried oxide layer. Finally, the buried oxide was removed through access holes to release the moveable portions of the microstructure from the substrate. Figure 2 shows a schematic of the finished wafer cross-section, the doping profiles, the current-voltage characteristics of the fabricated junctions, and the scanning electron microscope images of a fabricated device.

In order to study the phenomena, a simple mechanical structure was designed. The device is essentially a clamped-clamped beam where, in order to increase the device sensitivity to inertial forces, additional mass was added to the center of the beam in the form of two rectangular winglets. The pn junction was placed near the base of the clamped end of the beam where the mechanical

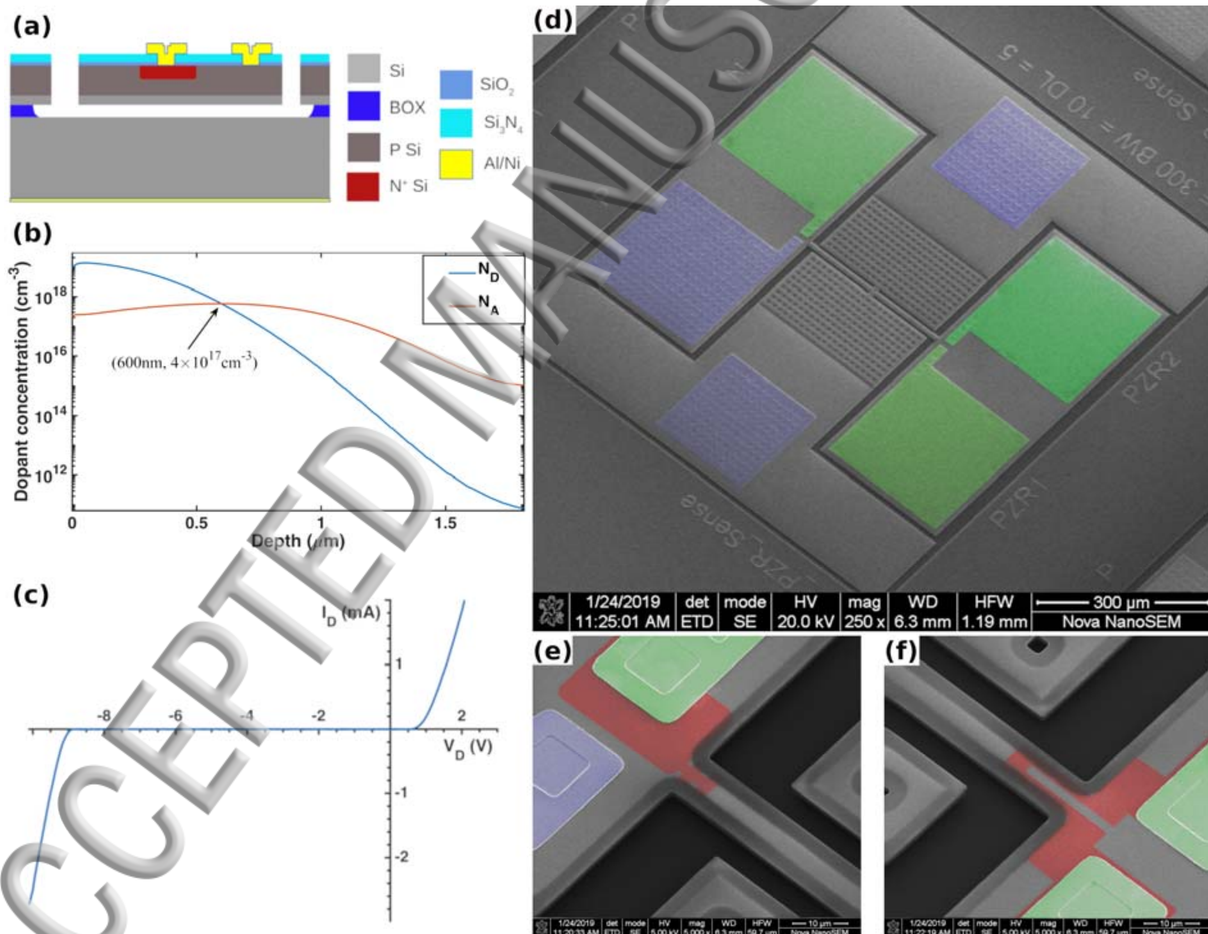

Figure 2. (a) Cross section of a finished wafer; (b) Doping profiles for boron (N_A) and phosphorous (N_D), forming the junction at 600nm below the surface; (c) Measured I-V characteristic of fabricated junctions; and (d) SEM of a partially released device where green and blue areas show metal contacts to the n-doped regions and p-type device layer, respectively; and Zoomed-in views of the piezo-avalanche (e) and piezoresistor (f) sensors embedded at the opposite ends of the mean beam.

ACCEPTED MANUSCRIPT

AIP Publishing

This manuscript was accepted by Appl. Phys. Lett. Click here to see the version of record.

stress due to beam deflections is at its highest. The beam was modeled using Euler-Bernoulli beam theory to estimate the mechanical stress for different input accelerations [27]. Estimated values of stress were verified through numerical simulations of the structure based on the finite element method. The variation of stress from the anchor point to the edge of active doping region (about 5µm into the released beam) was found to be within 5%. For the experiments, we thus assumed a uniform stress distribution across the pn junction. An implanted piezoresistor was also realized at the opposite clamped end of the beam during the fabrication process from junction-isolated doped regions. This piezoresistor, due to the device symmetry, is subjected to the same stresses during experiments and provides an independent way of stress measurement.

To evaluate the piezo-avalanche effect, the device was placed on a mechanical shaker and subjected to various inertial forces. Employing inertial forces avoids many potential challenges (e.g., interference and uncertainties) of other methods of applying forces to microstructures, such as using probes for atomic force microscopy or electrostatic actuation. The schematic for the experimental setup of piezo-avalanche sensor is shown in Figure 3. The junction of the device is reverse-biased with a source-measure unit used as a constant current source to force the junction

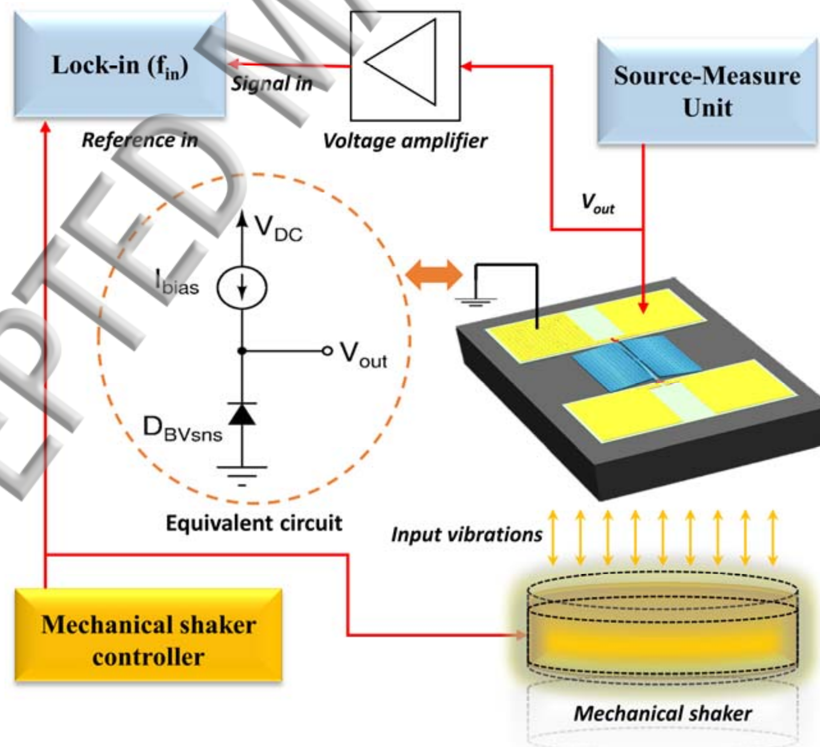

Figure 3. Test setup for piezo-avalanche measurements with a mechanical shaker.

ACCEPTED MANUSCRIPT

AIP Publishing

This manuscript was accepted by Appl. Phys. Lett. Click here to see the version of record.

into its breakdown region. The device is then mounted on the shaker for closed-loop tests where both the amplitude and frequency of vibrations were monitored in real-time using a reference accelerometer. Variations in the breakdown voltage were pre-amplified using an AC-coupled amplifier with a high-pass corner frequency of about 10Hz. The signal was then monitored on a lock-in amplifier that was synchronized to the analog command signal for the shaker.

Figure 4 depicts the device response to mechanical stress. In the experiment, the bias current through the junction was set to $I_{bias} = 500\mu A$ while the shaker was run at $500Hz$. This frequency is high enough so that the voltage amplifier will not block the signal while it is also small compared to the fundamental resonant frequency of structure at $20.3kHz$. The stress applied to the junction was calculated from acceleration amplitudes and structural models for the device. For input accelerations in the range of $1g$ to $10g$ ($1g \approx 9.8m/s^2$), the corresponding stresses ranged from

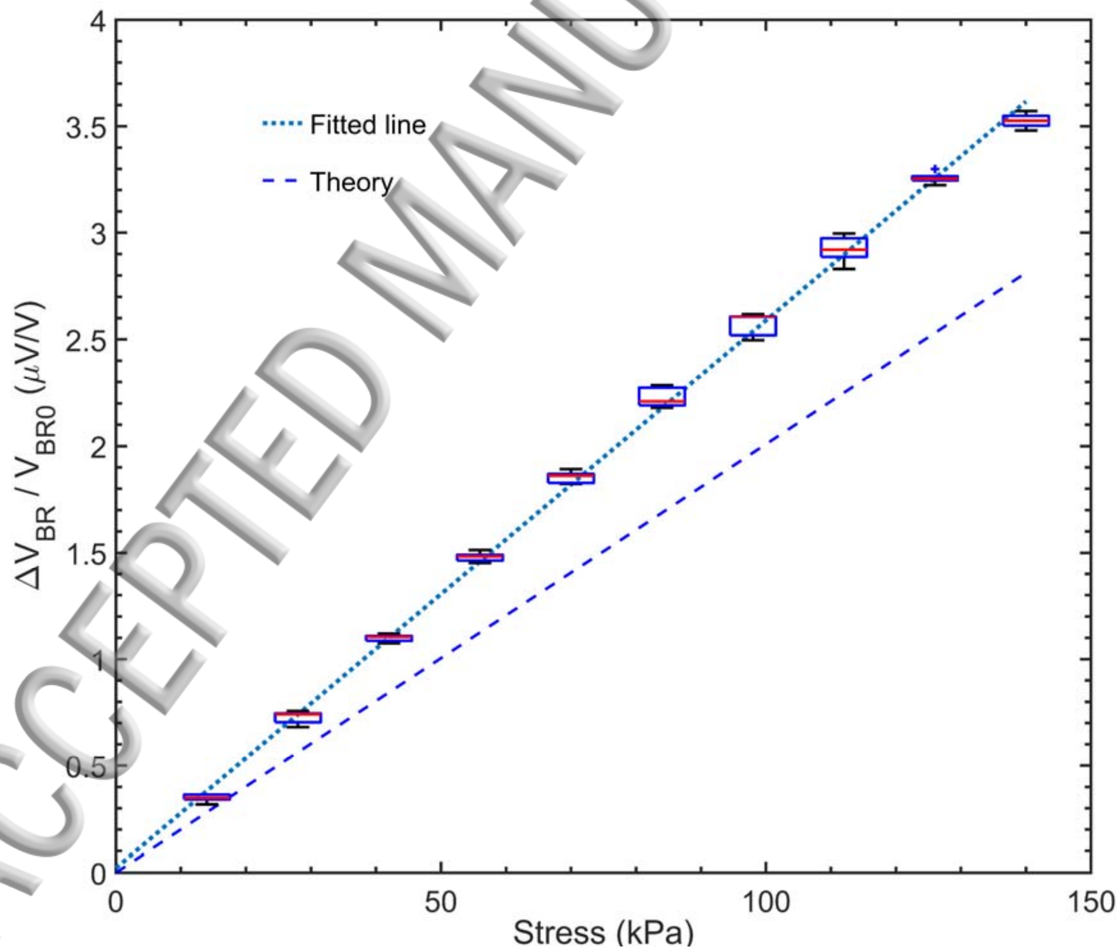

Figure 4: Comparison of the measurements for the dependence of breakdown voltage on mechanical stresses versus theoretical expectations at a bias current of $500\mu A$.

ACCEPTED MANUSCRIPT

AIP Publishing

This manuscript was accepted by Appl. Phys. Lett. Click here to see the version of record.

$14kPa$ to $144kPa$. The experiment was repeated over several days to ensure repeatability. As can be seen, the sensor response is linear and a direct function of the input stress. The piezo-avalanche sensitivity was estimated from the measurements to be around $235\mu V/MPa$ which is in good agreement with the predicted theoretical value of $240\mu V/MPa$.

Figure 5 shows the variations in the sensitivity of the piezo-avalanche effect as a function of the bias current for the junction. As can be seen, the device exhibits higher sensitivity at lower currents at the expense of increased noise. Both the breakdown voltage and device sensitivity become stable for bias currents larger than $\sim 400\mu A$ for this device.

The current in the junction increases exponentially for reverse voltages higher than the breakdown voltage of the device due to the avalanche effect [23]. This provides an opportunity for an alternative method for the measurement of the mechanical stresses where the diode may be biased within its breakdown region using a voltage source while monitoring the changes in current through the device in response to the stress. To demonstrate this approach, the diode was biased with a voltage source until a $500\mu A$ current flew through it at rest (i.e., $V_{BR0} = -9.345V$). The same amount of current was also flown through the piezoresistor at the opposite end of the beam

ACCEPTED MANUSCRIPT

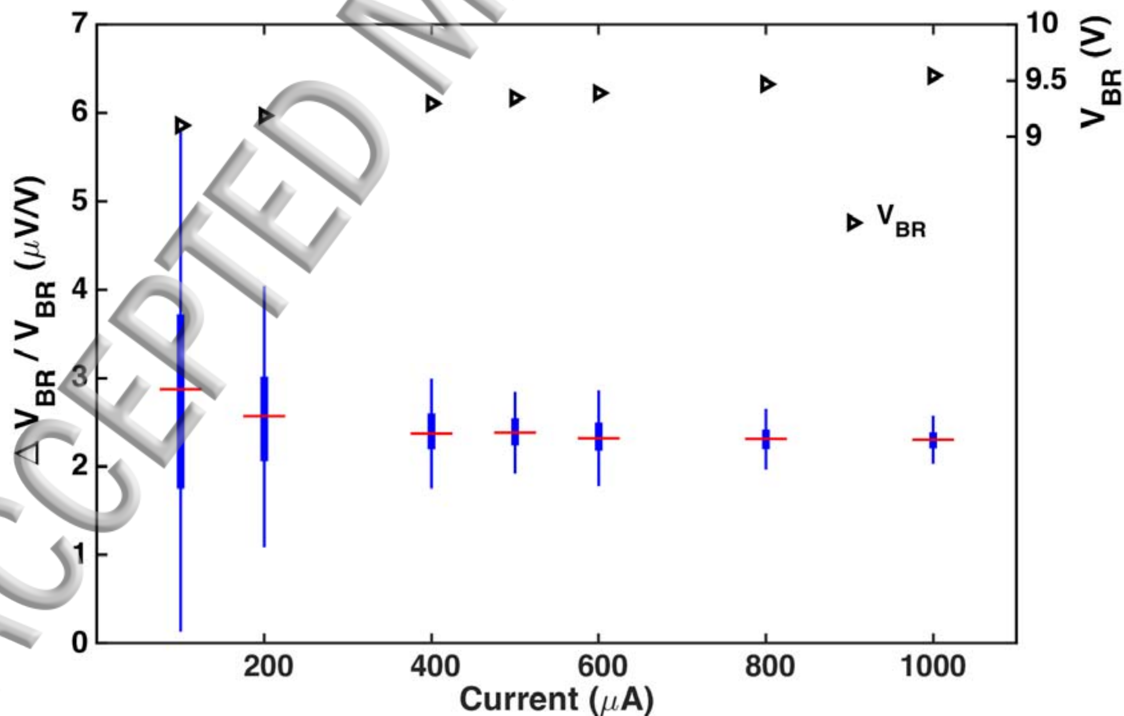

Figure 5: Variations in breakdown voltage and device sensitivity with bias current.

AIP Publishing

This manuscript was accepted by Appl. Phys. Lett. Click here to see the version of record.

($R_0 = 6.9k\Omega$). The device was then placed on the shaker and subjected to various magnitudes of inertial forces at $500Hz$. Figure 6 shows the measurement results for this experiment. As can be seen, the piezo-avalanche method offers a significantly higher sensitivity (~8.6 ×) in terms of the change in the current through the device. These results can be compared against the data obtained by using a current source to bias the diode or piezoresistor (i.e., the setup in Figure 3). While the voltage sensitivity of the breakdown voltage changes was $\sim 240\mu V/MPa$, the piezoresistor exhibited a higher voltage sensitivity of $\sim 330\mu V/MPa$ for the same bias current of $500\mu A$. This difference in performance between the two sensing methods (i.e., biasing with current and measuring voltage against biasing with voltage and measuring current) is due to the exponentially nonlinear current-voltage relationship of the diode compared to that of a linear resistor. This further

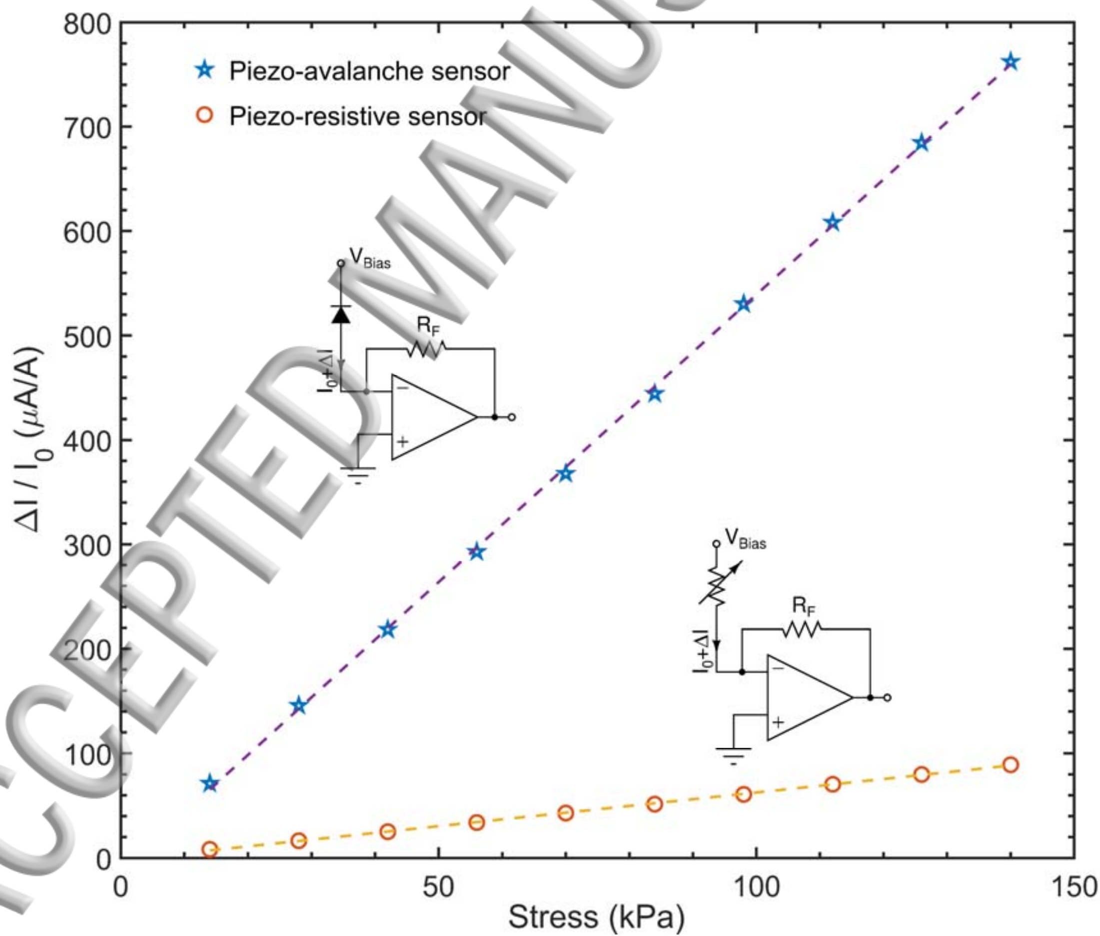

Figure 6: Comparison of the current sensitivity between the piezo-avalanche and piezoresistive sensing methods. The circuit above the data for each measurement replaces the SMU and voltage amplifier combination in Figure 3.

ACCEPTED MANUSCRIPT

AIP Publishing

This manuscript was accepted by Appl. Phys. Lett. Click here to see the version of record.

highlights the potential for developing sensors with significantly higher (and controllable) sensitivities compared to existing linear piezoresistive (and piezojunction) sensors.

The breakdown mechanism in pn-junctions has long been employed to build devices that operate continuously such as voltage references or avalanche photodiodes. While neither of the junction breakdown mechanisms are destructive on its own, the relatively large voltage drop across a junction brings up the possibility of permanent damage if the current is not limited externally. In practical implementations of sensors that employ the breakdown mechanism proper feedback mechanisms can be added to the interface circuit to avoid potential damage to the junction.

In summary, we demonstrated the use of the piezo-avalanche effect for the measurement of mechanical stresses at small scales. We further developed the theory behind the phenomenon, which was later verified experimentally. It was demonstrated that piezo-avalanche effect could offer a significantly higher sensitivity to stress compared to piezoresistive measurements. Moreover, compared to the piezoresistors, the piezo-avalanche effect is better suited for miniaturization due to the single-path measurement technique (i.e., measurement of a voltage compared to measurement of a resistance). This makes it possible to apply this method for strain measurement at nano-scales. On the other hand, the sensitivity of the method is higher at smaller bias currents at the expense of increased noise. This further allows for sensitive designs where the noise may be reduced through various averaging methods.

The research was supported by the Natural Sciences and Engineering Research Council of Canada under grant RGPIN-2014-04502. The authors acknowledge the use of microfabrication facilities at SFU 4D LABS and access to microdevice development tools through CMC Microsystems.

ACCEPTED MANUSCRIPT

AIP Publishing

This manuscript was accepted by Appl. Phys. Lett. Click here to see the version of record.

REFERENCES

[1] J. Fraden, *Handbook of Modern Sensors: Physics, Designs, and Applications*, 4th ed. (Springer-Verlag, New York, 2010).

[2] A.A. Barlian, W. Park, J.R. Mallon, A.J. Rastegar, and B.L. Pruitt, Proceedings of the IEEE **97**, 513 (2009).

[3] B. Yaghootkar, S. Azimi, and B. Bahreyni, IEEE Sensors Journal **17**, 4005 (2017).

[4] B. Bahreyni, F. Najafi, and C. Shafai, Sensors and Actuators A: Physical **127**, 325 (2006).

[5] J.F. Creemer, F. Fruett, G.C.M. Meijer, and P.J. French, IEEE Sensors Journal **1**, 98 (2001).

[6] D. Weinstein and S.A. Bhave, Nano Lett. **10**, 1234 (2010).

[7] D. Grogg and A.M. Ionescu, IEEE Transactions on Electron Devices **58**, 2113 (2011).

[8] A. Rasouli and B. Bahreyni, IEEE Transactions on Electron Devices **63**, 4452 (2016).

[9] E. Simoen, G. Eneman, M.B. Gonzalez, D. Kobayashi, A.L. Rodríguez, J.-A.J. Tejada, and C. Claeys, J. Electrochem. Soc. **158**, R27 (2011).

[10] J.J. Wortman, J.R. Hauser, and R.M. Burger, Journal of Applied Physics **35**, 2122 (1964).

[11] R. Edwards, IEEE Transactions on Electron Devices **11**, 286 (1964).

[12] Guin, Laurent, Jabbour, Michel, and Triantafyllidis, Nicolas, in (AFM, Association Française de Mécanique, 2017).

[13] Y. Kanda, Jpn. J. Appl. Phys. **6**, 475 (1967).

[14] S. Dhar, E. Ungersbock, H. Kosina, T. Grasser, and S. Selberherr, IEEE Transactions on Nanotechnology **6**, 97 (2007).

[15] K. Uchida, T. Krishnamohan, K.C. Saraswat, and Y. Nishi, in *IEEE International Electron Devices Meeting* (2005), pp. 129–132.

[16] I. Goroff and L. Kleinman, Phys. Rev. **132**, 1080 (1963).

[17] Y. Sun, S.E. Thompson, and T. Nishida, Journal of Applied Physics **101**, 104503 (2007).

[18] Y. Kanda, IEEE Transactions on Electron Devices **29**, 64 (1982).

[19] Y. Wu, A.R. Chew, G.A. Rojas, G. Sini, G. Haugstad, A. Belianinov, S.V. Kalinin, H. Li, C. Risko, J.-L. Brédas, A. Salleo, and C.D. Frisbie, Nature Communications **7**, 10270 (2016).

[20] P.M. Solomon, I. Lauer, A. Majumdar, J.T. Teherani, M. Luisier, J. Cai, and S.J. Koester, IEEE Electron Device Letters **32**, 464 (2011).

[21] E. Chan, D. Lin, L. Lu, D. Zhang, S. Guo, Y. Zhang, K. Chau, and M. Wong, Journal of Microelectromechanical Systems **27**, 231 (2018).

[22] J.F. Creemer and P.J. French, Sensors and Actuators A: Physical **97–98**, 289 (2002).

[23] S.M. Sze and M.-K. Lee, *Semiconductor Devices: Physics and Technology*, 3 edition (Wiley, Hoboken, N.J, 2012).

[24] A. Goetzberger and R.H. Finch, Journal of Applied Physics **35**, 1851 (1964).

[25] W. Rindner, Appl. Phys. Lett. **6**, 225 (1965).

[26] J.L. Hudgins, G.S. Simin, E. Santi, and M.A. Khan, IEEE Transactions on Power Electronics **18**, 907 (2003).

ACCEPTED MANUSCRIPT

This manuscript was accepted by Appl. Phys. Lett. Click here to see the version of record.

[27] B. Bahreyni, *Fabrication and Design of Resonant Microdevices* (William Andrew Publishing, New York, USA, 2008).

ACCEPTED MANUSCRIPT

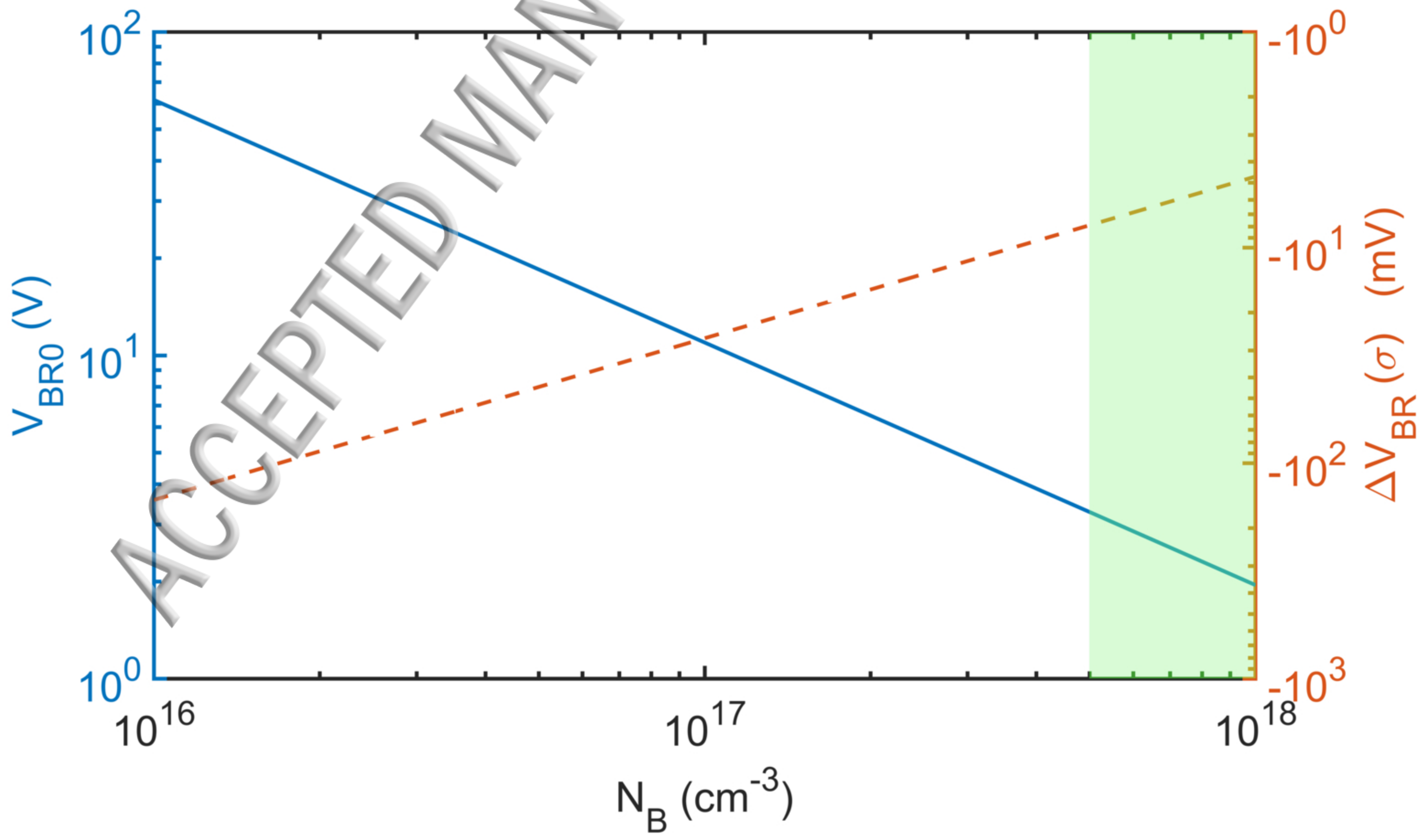

ACCEPTED MAN

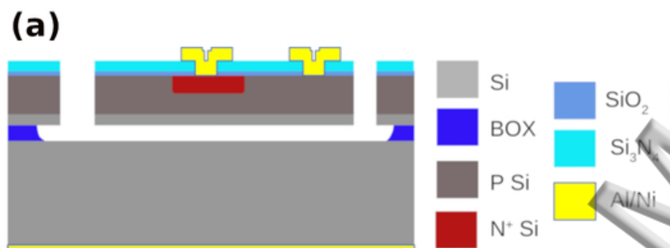

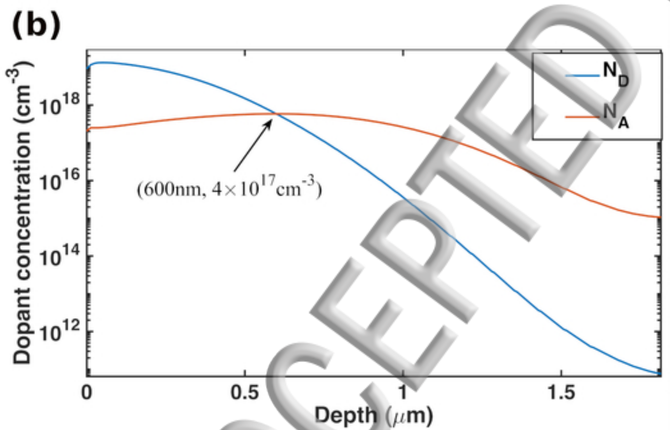

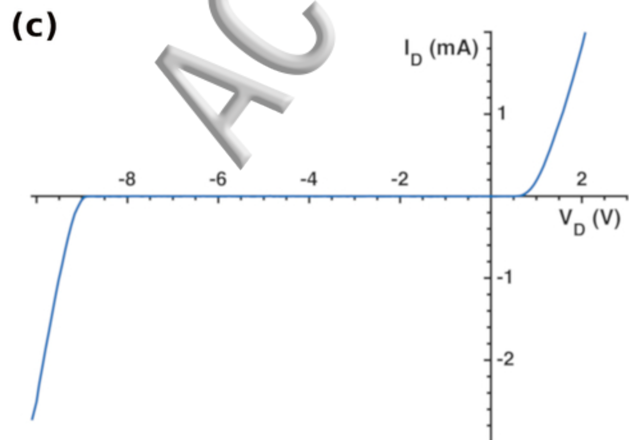

(d)

N

P

PZR2

PZR1

PZR_Sense

1/24/2019 11:25:01 AM | det ETD | mode SE | HV 20.0 kV | mag 250 x | WD 6.3 mm | HFW 1.19 mm | 300 μm | Nova NanoSEM

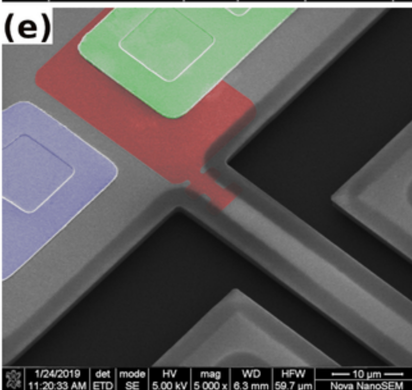

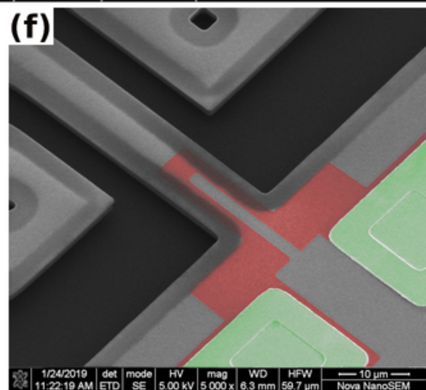

ACCEPTED MANUSCRIPT

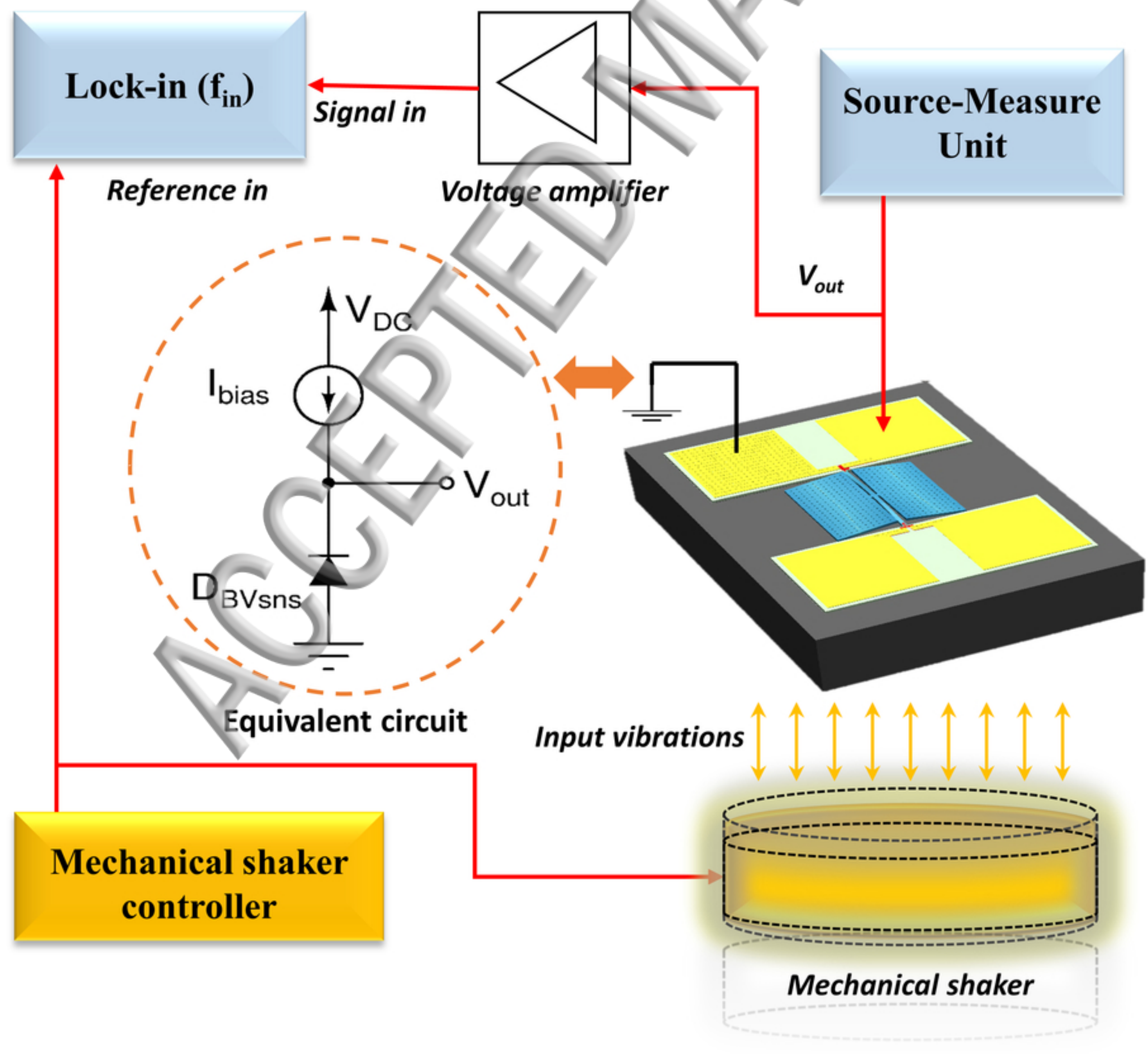

ACCEPTED MANUSCRIPT

Publishing

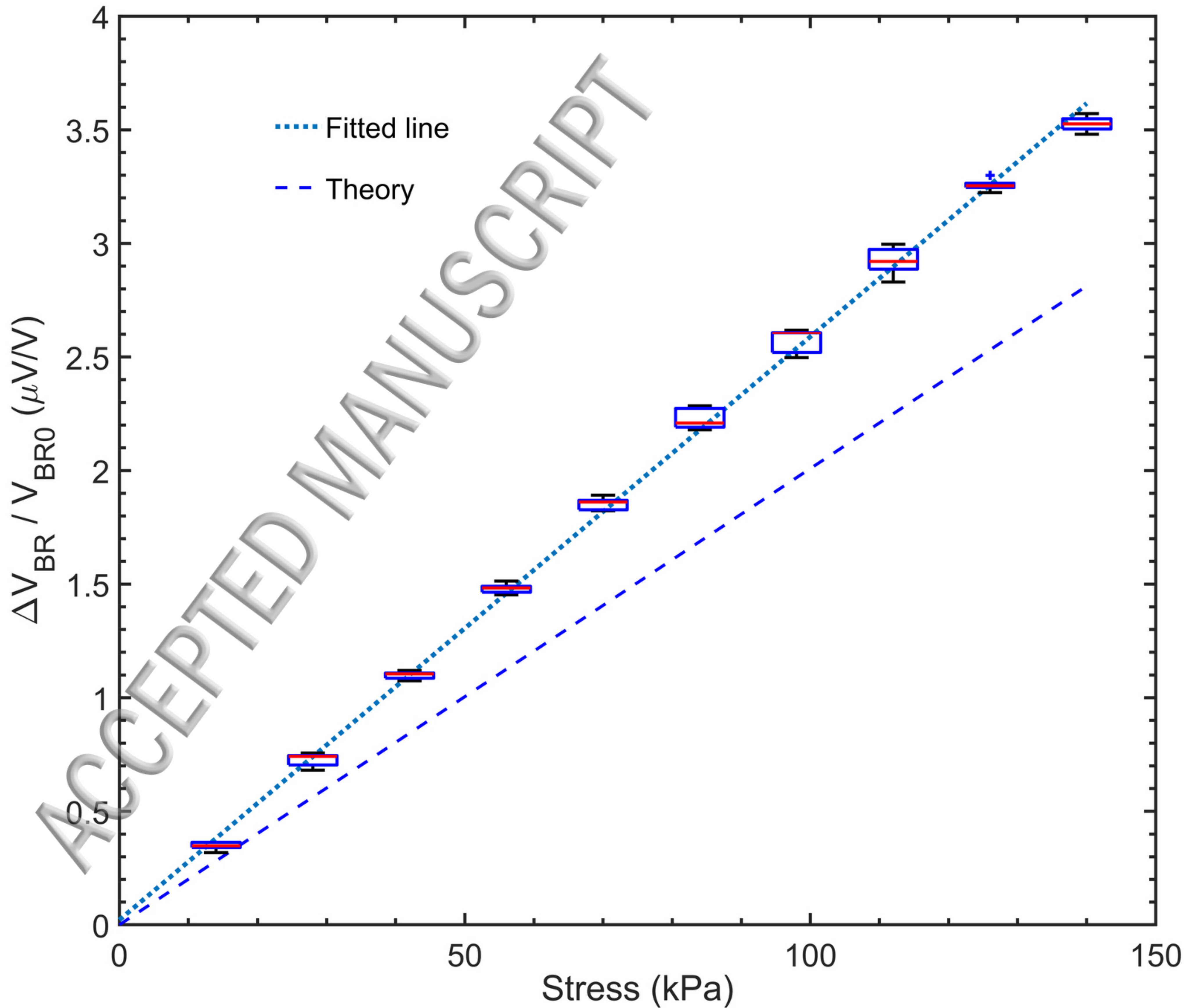

ACCEPTED MANUSCRIPT

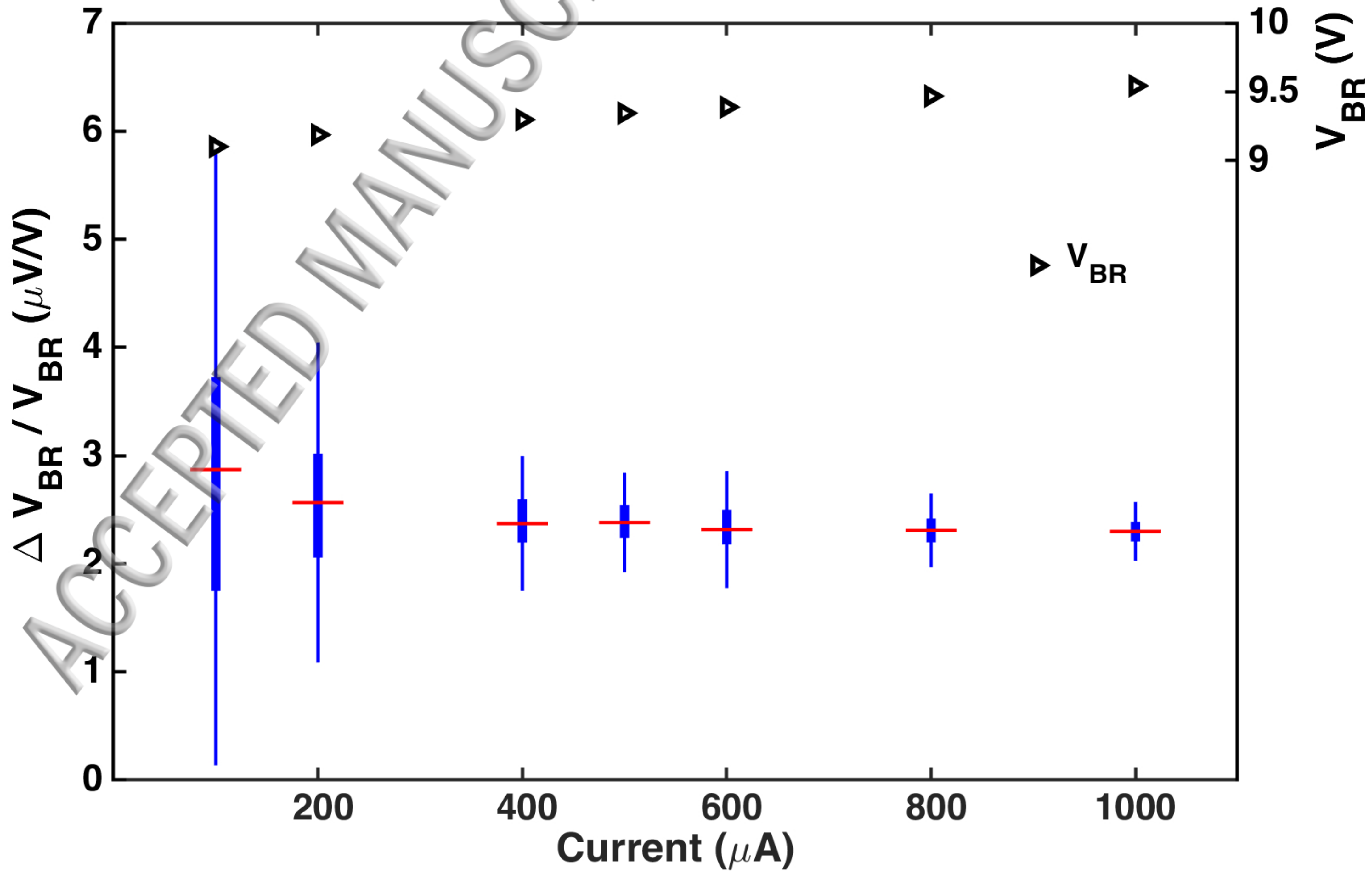

ACCEPTED MANUSCR

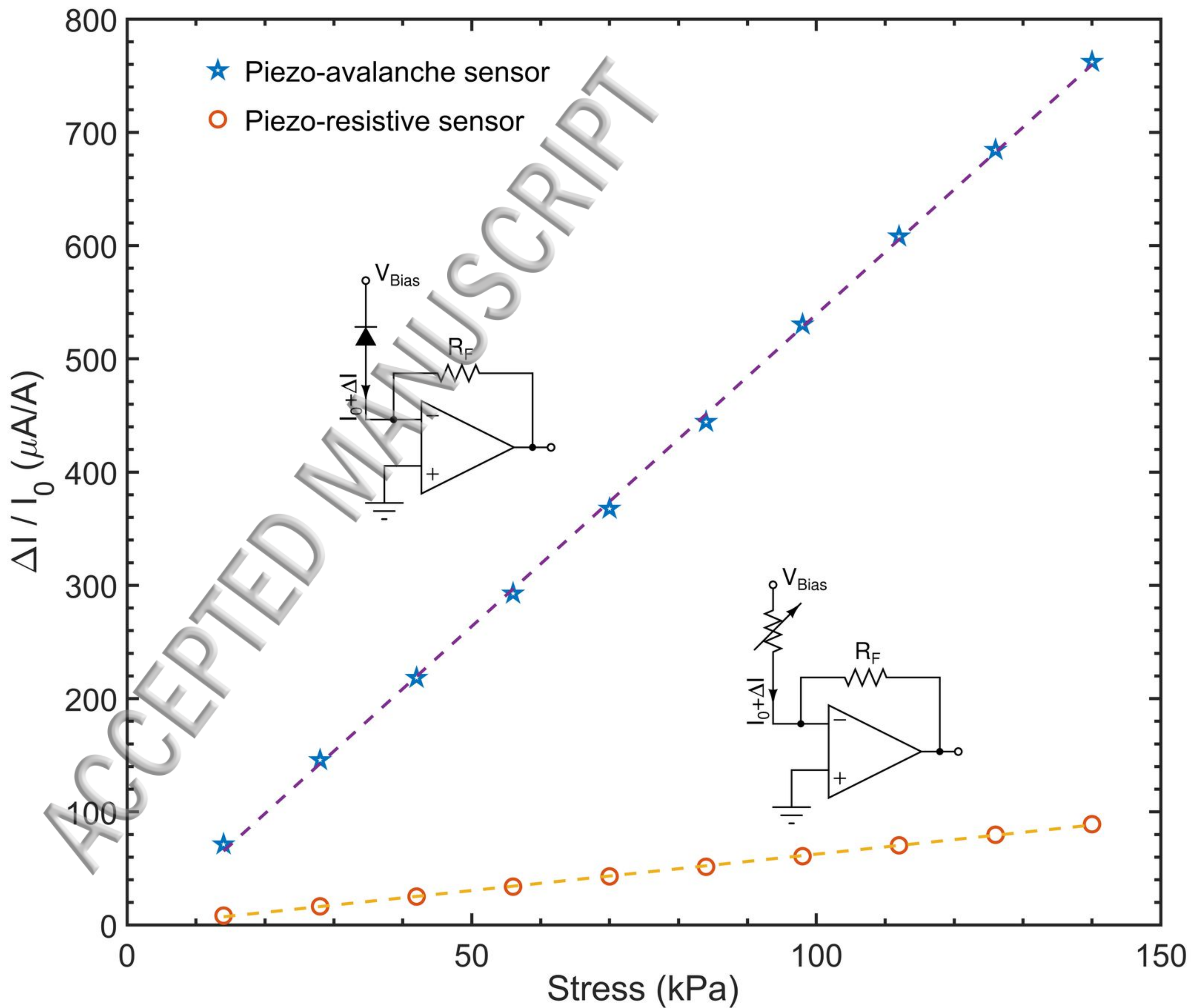

ACCEPTED MANUSCRIPT